COBEM 99
XV Congresso Brasileiro de Engenharia Mecânica
15th Brazilian Congress of Mechanical Engineering
22 - 26 de Novembro de 1999 / November 22 - 26, 1999 Águas de Lindóia, São Paulo,

VIBRATION IN THE CAT MIDDLE EAR

Willem F. Decraemer
University of Antwerp, RUCA
Biomedical Physics Department, Groenenborgerlaan 171 – Antwerpen, B-2020, Belgium
Shyam M. Khanna
Columbia University
Dept. Otolaryngology, 630 West 168th Street, New York, NY 10032, USA
W. Robert J. Funnell
McGill University
Montreal, Canada

Abstract. *The acoustical energy is transmitted from the tympanic membrane to the inner ear by the middle ear ossicles. It is accepted that the ossicles rotate around a fixed axis and function as mechanical levers. Measurements of malleus vibration has clearly shown that its motion is not a rotation about a fixed suspension axis but that translation and rotation components in all three dimensions are present and change dramatically over the frequency of hearing.*
The question arises how complex is the motion of the stapes? The motion of the stapes has been difficult to measure because access is limited and the crura can only be seen partially. In order to get a better access a novel temporal bone preparation was utilized.
The vibration of the stapes was measured with a confocal heterodyne interferometer at three points from different viewing angles. Its geometry was also measured. Rigid body motion can be decomposed in a global translation and a rotation about an immediate rotation axis. The three dimensional components of the stapes motion are presented in this paper. Our results show that the motion is largely piston-like, but other, small, components that will cause tilting of the footplate are also present.

Keywords: *Middle ear, Mechanics, Ossicles, Vibration, Interferometer*

1. INTRODUCTION

The function of the middle ear is in most textbooks described as that of an impedance transformer between the low input impedance of the middle ear at the air-tympanic membrane interface (large displacement velocity combined with small pressure) and a high output impedance at the stapedius footplate-perilymph interface (small displacement velocity combined with large pressure). The ossicles in this hypothesis rotate as a lever system about a fixed axis which in cat runs through the cranial anchorage of the anterior process of the malleus and the end of the short process of the incus. As a consequence the stapes should vibrate almost as a piston in the oval window and all points on the the manubrium of the malleus should vibrate in phase.

The motion of the stapes defining the middle ear output was studied by different authors in man and in various species. In human (Kobrak(1959), von Békésy (1960) and Kirikae (1960)) describe the stapes motion as a rotation about an axis, the position of which differed however in the different studies. More sophisticated and more recent measurements (Dankbaar (1970), Gundersen (1972), Cancura (1976), Høgmoen and Gundersen (1977), Feenstra and Vlaming (1987)) agree on a predominantly piston-like movement of the stapes footplate. Some authors mention a supplementary rotational movement but with significantly smaller displacement.

In cat only Guinan and Peake (1967) measured the stapes motion in great detail using stroboscopic microscopy. It was found that to a good approximation the footplate has a piston-like motion. We have clearly shown in a series of papers that the malleus of cat does not vibrate according to the fixed axis hypothesis (Decraemer and Khanna 1994, 1995, 1997) but that the motion is varying from frequency to frequency and that all 3-D components of translational and rotational vibration are present. A fixed rotation axis at a given frequency is generally not seen. The immediate rotation axis does not remain fixed within a cycle. This strongly deviating view of the malleus vibration and especially it complexity motivated us to investigate also the motion of the stapes. As in our studies of malleus vibration we did not assume any preferential direction of stapes motion but measured the full 3-D components of the stapes vibration at three points, one at the stapes head and two on the two respective crura, and calculated herewith the 3-D rigid body motion of the stapes. From these measurements the frequency responses for three dimensional rotation and translation components were determined.

.

2. MATERIAL AND PREPARATION

The view of the stapes is severely obstructed by parts of the incus and malleus and suspending ligaments and by the tympanic cavity wall that forms a niche that houses the footplate and the lower half of the crura. To obtain good access to stapes that allows both good visualization and good incidence for interferometric measurements we had to recur to measurements on fresh temporal bones.

The experiments were performed on temporal bones from cats weighting between 1.9 and 2.5 kg. After the cats were put asleep both temporal bones were extracted and examined. Only middle ears with clear tympanic membrane and without any bleeding in the middle ear cavity were used. Using the small temporal bone preparation allowed us to choose either the left or right ear for the measurements. The most complete data set that will be used in this paper was recorded from a left ear. The external ear is mostly removed leaving about 1 cm of the end of the external ear canal. A tight fitting conical ear insert is placed in the remaining ear canal. An acoustic transducer with a probe microphone is coupled to this insert to apply sound and measure its pressure (Stinson and Khanna, 1994).

The middle ear cavity is opened form the ventral side near the place were the base of the conical tensor tympani muscle is attached to the middle ear wall. The muscle ligament attached to anterior process (AP) of the malleus handle is cut and removed. When the whole is further enlarged we obtain a good aperture to the stapes head and upper part of both crura (Fig. 1). The lower part of the crura and the footplate of the stapes remain hidden behind a bony rim and vibration measurements could not be obtained there.

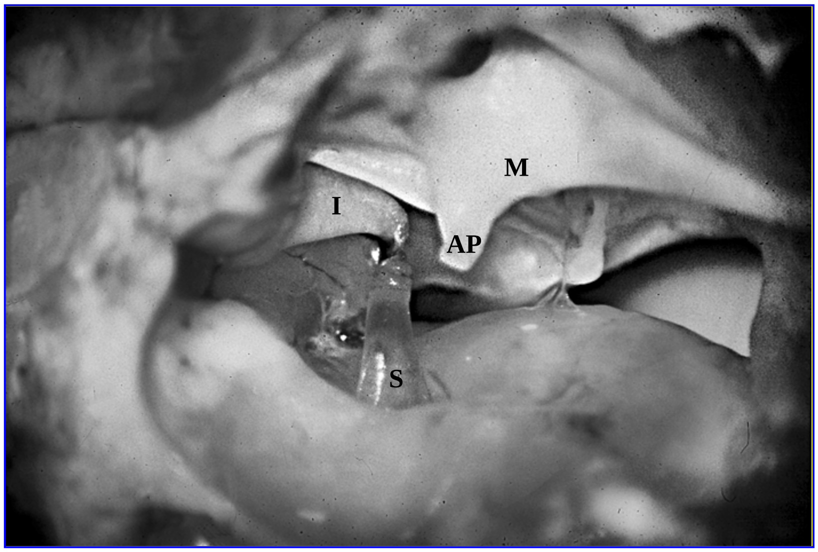

Figure 1 - Picture of the middle ear of a cat taken through the opening made in the wall of the middle ear. We recognize from top to bottom first the white structure as the malleus (M) with the anterior process (AP) pointing to the camera (the ligament was severed), then part of the incus (I) and stapes (S) with its front and rear leg. The footplate is hidden in a bony niche.

When the middle ear is opened and the medial mucous side of the tympanic membrane is exposed to the air, it quickly dries out. This is a well know problem in middle ear research. We provide humidity in the middle ear by placing tiny pieces of wet paper towel on the floor of the middle ear cavity and resealed the middle ear cavity with a microscope cover slip,. It was held with a ring of soft modeling clay pressed around the cavity opening. To equalize pressure differences between the middle ear cavity and the ambient room a small capillary tube (PE 10, length 6 cm) is conducted through the modeling clay. This novel middle ear preparation has the advantage that the middle ear cavity is closed during the measurements and minimally altered in volume. The bony septum is also kept in place. The total preparation time was of the order of three hours.

3. EQUIPMENT AND MEASURING PROCEDURE

The temporal bone is glued with dental cement onto a rigid plastic tube (3m long, 1cm diameter) which is then used to mount the specimen in the microscope-interferometer. The clamp allows many degrees of freedom so that the object can be positioned so that both crura and the head of the stapes are visible (Fig. 1). The object mounting system of the interferometer is suspended within two nested goniometers. They allow to change the observation angle of any selected point in two orthogonal planes by rotation of the object around the focal point (Decraemer and Khanna, 1994). Three translation stages equipped with micrometer reading scales allow to change the observation point and to record the x,y,z coordinates precisely. Stepper motors that can be controlled from a computer activate the two rotations and the three translations. The acoustic system and the temporal bone are mounted on the same post and move together as the position or the observation direction is changed. The measuring equipment and procedure has been described previously (Decraemer et al 1991).

The interferometer is first focused on a point on the head of the stapes, about a tenth of a mm below the incudo-stapedial joint. Using pure tone stimuli with reasonably moderate sound pressures (between 80 and 90 dB) frequency responses are repeatedly measured with the heterodyne interferometer at this same position until we get a stable response.

For a large number of frequencies vibration was measured at 3 points P_i (i=1,3) one at the stapes head and one at the base of each of the crura using different viewing angles by changing the goniometers positions in small increments. Sound pressures are measured simultaneously.

4. METHOD

4.1 Rigid body motion

To describe the motion of a rigid body mathematically we will use a stationary, inertial reference frame O_{xyz}. The general motion of a rigid body may be decomposed in a rotation about the origin O followed by a global translation of the body. Consequently the velocity of a point P_i of the rigid body (stapes) can be written as

$$\mathbf{v_i(t)=v_t(t)+\Omega(t)\times r_i} \qquad (1)$$

$\mathbf{v_i(t)}$: velocity of P_i with components v_x, v_y, v_z
$\mathbf{v_t(t)}$: velocity of the global translational motion component, with components $v_{O'x}$, $v_{O'y}$, $v_{O'z}$
$\mathbf{\Omega(\tau)}$: angular velocity of the rigid body rotating about O with components Ω_x, Ω_y, Ω_z
$\mathbf{r_i}$: rest-position vector of point P_i with components x, y, z.
$\mathbf{\Omega(t)\times r_i}$: velocity of the rotational motion component of P_i relative to O_{xyz}

In our experiments we use a harmonic sound stimulus and as a consequence all functions of time t become harmonic.

We can write **v** as **ds**/dt and **dΩ** as **dΘ**/dt so that multiplying both sides of eq. (1) by dt we end up with an equation between infinitesimal linear and angular displacements

$$\mathbf{ds_i t)=ds_t(t)+ d\Theta(t)\times r_i} \qquad (2)$$

The middle ear vibration amplitudes are small (of the order of 10^{-8} m) so that eq. (2) can be used to describe the experimental displacements. In what follows the differential notation will be further used to denote very small but finite displacements.

4.3 Determination of the rigid body motion

Step 1 : Calculation of the three-dimensional motion of the three observation points

The measurements obtained at each of the 3 observation points are separately used to compute the amplitude and phase for the x, y and z component of the displacement of the given point following a procedure outlined in an earlier paper (Decraemer et al. 1994 b).

Step 2 : Three-dimensional rigid body motion of the stapes

The 3-D motion components for all points P_i at a given frequency are then utilized in a subsequent numerical fitting procedure to reconstruct the 3-D rigid body motion of the stapes. This fit determines the amplitude and phase of $\mathbf{v}_t\mathbf{(t)}$ and $\mathbf{\Omega(t)}$ which describe the rigid body motion as shown in Eq. 1. This procedure is repeated for each experimental frequency (Decraemer and Khanna, 1996, 1997).

5 RESULTS

5.1 Choice of observation points

We have measured the vibration of the stapes at three points, spread out from each other as far as possible: one point at the head of the stapes, the other two points as low as possible on the front and the rear leg. The position of these points in the image plane as seen during the experiment is shown as thick dots in fig. 2. On the same plot we show the points measured on the stapes, incus and malleus used to record the overall geometry of the middle ear ossicles. The observation direction for the interferometer is along the z-axis. Following the procedure outlined above the 3-D components of the 3 observation points were calculated. The 3 harmonically time varying displacement vectors thus obtained served subsequently as input for the fit that determines frequency per frequency the amplitude and phase of $\mathbf{v}_t\mathbf{(t)}$ and $\mathbf{\Omega(t)}$ which fully describe the rigid body motion (Eq. 1).

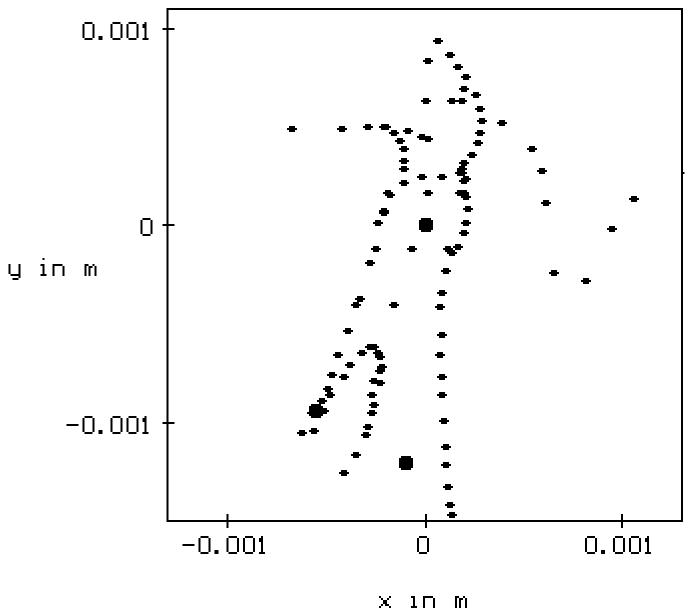

Figure 2 - The three observation points on the stapes (thick dots) and some points to outline geometry of the stapes, incus and malleus (finer dots).

5.2 From the experimental to an intrinsic coordinate reference system for the stapes

The amplitudes and phases of $\mathbf{v}_t\mathbf{(t)}$ and $\mathbf{\Omega(t)}$ are very hard to interpret as the orientation of the stapes with respect to the experimental reference system is arbitrary and determined by the accessibility to the stapes during the experiment (Fig. 1). It is possible to apply a coordinate transformation to bring the stapes in an intrinsic reference system. This transformation brings the stapes from the experimental position shown in Fig. 4a into the position in the intrinsic reference system shown in Fig. 4b.

The simplified stapes model shown in Fig. 4b was obtained from two images of an isolated cat stapes in an upright position taken from the front (perpendicular to the plane of the two legs, as in Fig. 4b) and after rotation over 90 degrees from the side (the front leg hiding the rear leg). Based on these images we have derived coordinates for 11 contours parallel to the footplate. We made use of the symmetry of the stapes with respect to the x,y plane and the y,z plane as defined in Fig. 4b. Each contour is defined with 30 points. The position of the lateral process was intentionally emphasized to serve as a landmark. The footplate in the present model is oversimplified as it lacks its upstanding rim. For our present purpose where this model only serves to visualize the stapes motion this is not important.

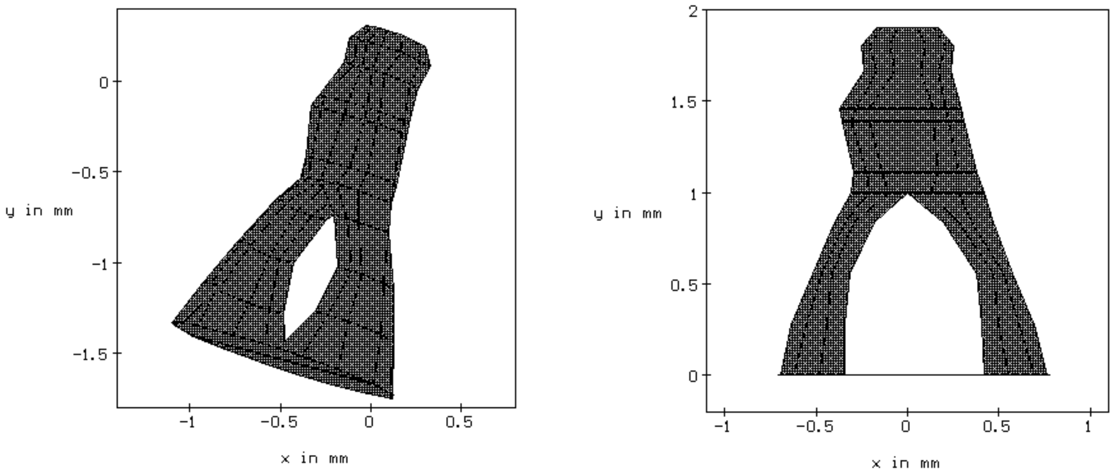

Figure 4 – A simplified model of the stapes constructed from two orthogonal views of the stapes. In the right panel (Fig. 4b) we see it in a frontal view. In the left panel (Fig. 4a) the model is rotated and translated to bring it in the position of the stapes in the temporal bone during the measurements described in this paper.

The parameters for the stapes transformation from the slanted to the upright position were determined using the anatomical measurements of the stapes taken during the experiments (finer dots in Fig. 2). Applying consecutive rotations about the x,y and z-axes of the experimental reference system, the stapes was brought in an upright position as in Fig. 4b. To complete the coordinate transformation the coordinate origin was finally translated to the center of the footplate. The final position and orientation of the stapes in the intrinsic reference system is best judged from Fig. 4b.

5.3 Frequency responses in the intrinsic coordinate reference system for the stapes

The coordinate transformation described in the previous section was applied to the components of the translation and rotation displacement. In this reference system these components can be quite well interpreted: the x and z rotation components are now rotations about the long and short axis of the elliptical footplate that will cause tilting of the footplate, the y-component is an in-plane rotation of the stapes footplate in the oval window. The x and z translation components are both in-plane translations for the footplate, the y-component is the out-of-plane motion. The final motion of the stapes is a combination of all these components were the phase differences between the components have to be taken into account.

Frequency responses for the translation components

The frequency responses for the translation components is shown in Fig. 5, the amplitude responses in the upper panel, the phase responses after unwrapping in the lower panel.

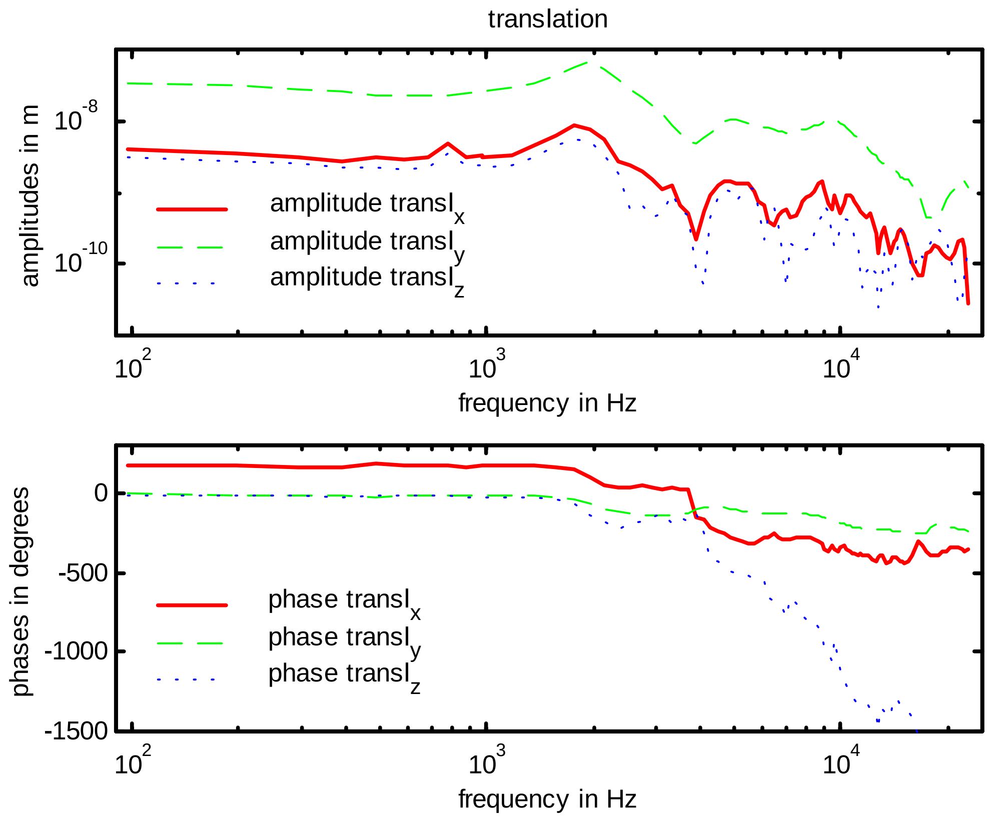

Figure 5 - Frequency responses for the x, y, and z components of the translation displacement part in the rigid body motion. The upper panel Fig. 5a shows the amplitudes as a function of frequency, the lower panel (Fig. 5b) the respective phases relative to the sound pressure.

The shape of the amplitude response curve is very comparable to that of points on the manubrium (Decraemer and Khanna (1991). The low frequency plateau, the resonance peak at about 2 kHz, the dip at 4 kHz due to the bulla cavity resonance, the roll-off at higher frequencies with a few fluctuations superimposed, it all is present in the stapes curve. The amplitude of the y-motion (the piston-like component) is one order of magnitude larger than the x- component (along the long axis of the footplate) and the z-component (along the short axis of the footplate) at most frequencies. The phase difference between the 3 components is at low frequencies 180 degrees and close to a multiple of 180 degrees at higher frequencies.

Frequency responses for the angular displacement

The rotation about the long axis of the footplate (x-axis) dominates the two other components up to 8 kHz. Above this frequency the x component decreases and the 3 amplitudes become more or less comparable. The 3 components remain almost perfectly in phase over the entire frequency range.

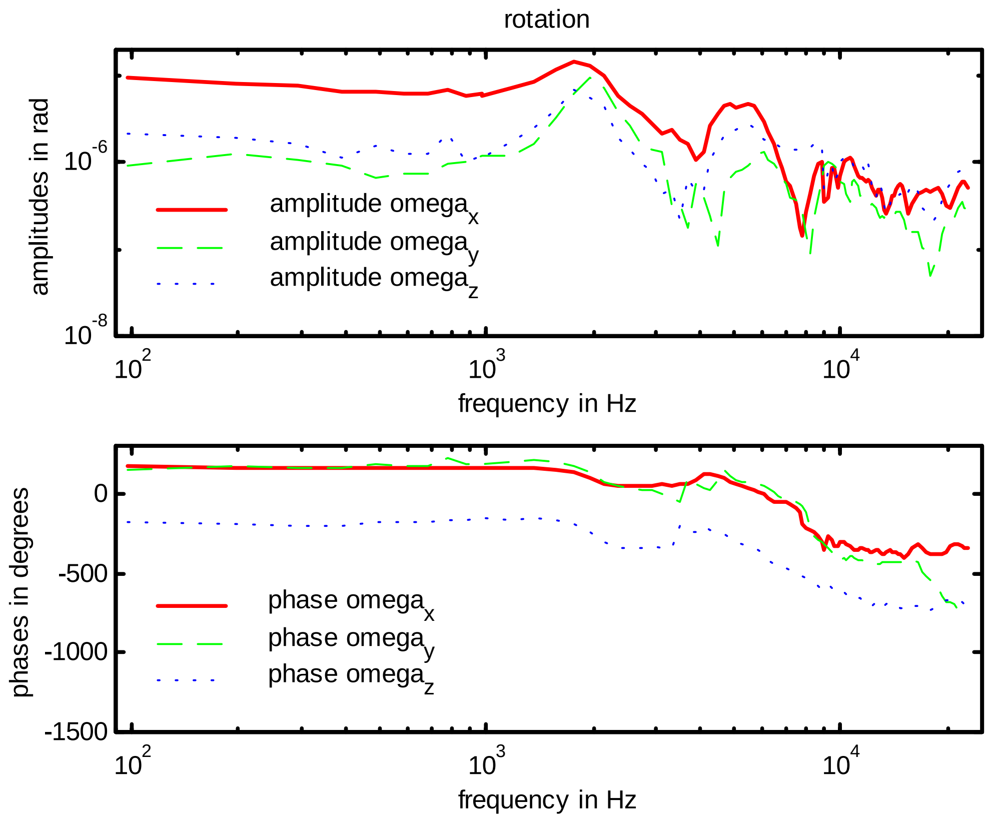

Figure 6 - Frequency responses for the x,y, and z components of the angular displacement of the rigid body motion. The upper panel Fig. 6a shows the amplitudes as a function of frequency, the lower panel (Fig. 6b) the respective phases relative to the sound pressure.

6. DISCUSSION

The present results are based on one complete set of 3-D measurements obtained on a single temporal bone. At all frequencies the motion of the stapes has a large piston-like component but other substantial components are also present. We will refrain from making strong statements about stapes motion before more data will be available.
The present measurement technique has made middle ear vibration measurements possible with the middle ear cavity closed and nearly intact thanks to a novel preparation. Measurements on the other ossicles have also to be made to get a compete description of middle ear motion. This is in principle possible with the actual preparation but the change of the response of the system, even for a temporal bone, is a factor limiting the amount of

data that can be collected. By further automating our measurement procedure we hope to solve this issue.

Acknowledgements

Research supported by Emil Capita Fund, NOSH, Fund for Scientific Research (Flanders, Belgium) and Research Funds of the University of Antwerp (RUCA).

REFERENCES

1. G. von Békésy (1960), *Experiments in hearing*, E.G. Wever, Ed., McGraw Hill Book Co., New York.
2. W.A. Dankbaar (1970), "The pattern of stapedial vibration", *J. Acoust. Soc. Am.* 48, 1021-22.
3. W.F. Decraemer, S.M. Khanna, W.R.J. Funnell (1991), "Malleus vibration mode changes with frequency," *Hearing Research*, 54, 305-318.
4. W.F. Decraemer, S.M. Khanna, W.R.J. Funnell (1994), "Modelling the malleus vibration as a rigid body motion with one rotational and one translational degree of freedom," *Hearing Research*, 72 1/2, 1-18.
5. W.F. Decraemer, S.M. Khanna (1994), "A method for determining three-dimensional vibration in the ear," *Hearing Research*, 77, 19-37.
6. W.F. Decraemer, S.M. Khanna (1996), "Malleus vibrations in the cat ear are three dimensional," *Proceedings of the Diversity in Auditory Mechanics*, *Berkeley*, California 115-121.
7. W.F. Decraemer and S.M. Khanna (1997), "Vibrations on the malleus measured through the ear canal," *Proceedings of Middle ear mechanics in Research and Otosurgery*, Dresden, September 19-22, 1996, Ed. K.B. Hüttenbrink, 32-39.
8. L. Feenstra and M.S.M.G. Vlaming (1987), "Laser interferometry with human temporal bones," *Adv. Oto-Rhino-Laryngol.* 37, 36-38.
9. J.J. Guinan an W.F. Peake, (1967), " Middle-ear characteristics of anesthetized cats," *J. Acoust. Soc. Am.* 41, 1237-1261.
10. T. Gundersen and K. Høgmoen (1976), "Holographic vibration analysis of the ossicular chain," Acta Otolaryng. (Stockholm), 82, 16-25.
11. H.G. Kobrak (1959), *The middle ear*, Univ. Chicago Press, Chicago.
12. J. Kirikae, (1960), *The structure and function of the middle ear*, Univ. Tokyo Press.
13. Stinson M.R., and Khanna S.M.(1994), "Spatial distribution of sound pressure and energy flow conditions in the ear canals of cats," *J. Acoust. Soc. Am* 96(1), 170-180.